FLOW IN THE ANNULAR FILM AROUND A TAYLOR BUBBLE RISING TROUGH VERTICAL COLUMNS OF LIQUIDS

S. NOGUEIRA [O]*, M. L. RIETHMULLER[O], J. B. L. M. CAMPOS*, A. M. F. R. PINTO*[#]

*Centro de Estudos de Fenómenos de Transporte, DEQ, Faculdade de Engenharia da Universidade do Porto

Rua Dr. Roberto Frias, 4200 - 465 Porto, Portugal, E-mail: nogueira@fe.up.pt, jmc@fe.up.pt., apinto@fe.up.pt

[o]von Karman Institute for Fluid Dynamics, Chaussée de Waterloo, 72 B-1640 Rhode Saint Genèse – Belgium

E-mail: nogueira@vki.ac.be , riethmuller@vki.ac.be

[#] Corresponding author

ABSTRACT

The flow in the annular film around individual Taylor bubbles rising trough stagnant and co-current vertical columns of liquid was studied employing simultaneously particle image velocimetry (PIV) and pulsed shadowgraphy (PST). This combined allows the simultaneous determination of the bubble interface position and the velocity profiles in the liquid film. Experiments were performed with aqueous glycerol solutions in a wide range of viscosities ($2x10^{-3}$ Pa.s < μ < 0.22 Pa.s), in an acrylic column of 32 mm I.D.

The results show that from the nose, the liquid film accelerates and below a certain distance stabilises in velocity and in thickness, becoming a free falling film. Values for the developing length and for the film thickness are reported for the experimental studied conditions. Average velocity profiles in the fully developed region are also presented. A critical Reynolds number (based on the mean absolute velocity in the liquid film) around 400 is reported for the transition from laminar to turbulent regime.

INTRODUCTION

Slug flow is a two-phase flow pattern observed when gas and liquid flow simultaneously in a pipe over a determined range of flow rates and is characterized by large bullet-shaped bubbles, also called Taylor bubbles or gas slugs, which nearly occupy the entire cross-section of the pipe. The liquid moves around the bubbles forming a thin film and in bulk between successive bubbles. The liquid confined between the bubble and the pipe wall separates at the rear of the bubble inducing a liquid wake.

This type of flow is found commonly in many practical applications such as gas absorption units, nuclear reactors, oil-gas pipelines, steam boilers, heat exchangers and air-lift reactors. Therefore, a great amount of research has been devoted to the study of this flow pattern since the early 1940s [1-12], the most important of which was reviewed in the work of Fabre and Liné [13].

In a slugging column, with flowing gas and liquid, the flow field is extremely complex. The detailed study of the entire flow field around the Taylor bubble is a fundamental step towards the hydrodynamic understanding of this type of two-phase flow pattern. As pointed out by Mao and Duckler, [9], there is still uncertainty concerning the velocity and shear stress boundary conditions at the gas-liquid interface. Experiments by these authors obtained with intrusive techniques suggest that the constant film thickness resulting from a fully developed velocity profile is never reached. This is in contrast with the work of Nicklin et al. [3] who observed a stabilised film (in velocity and thickness) below a certain distance from the bubble nose. None of the model predictions on the velocity field around the Taylor bubble has been experimentally validated since there is a lack of quantitative velocity profile measurements in the liquid surrounding the bubble, namely in the annular liquid film.

It should be mentioned the work of Polonsky et al. [14] who studied the motion of an isolated gas slug rising in a vertical pipe filled with water, for different liquid flow rates. They used an interlaced image technique to perform Particle Image Velocimetry (PIV) measurements around the nose of the gas slug. Due to the higher liquid velocities in the annular film around the gas slug, they had to use a streak length method. Van Hout et al. [15] performed PIV measurements in slug flow for air-water systems, for stagnant water in the pipe. They determined, separately, the shape of the Taylor bubble, using the same procedure as Polonsky et al. [14]. With the technique used, the authors had problems to determine accurately the velocity field both in the liquid film and in the near-wake region. Bugg and Saad [16] studied the flow around a Taylor bubble rising in a viscous solution. Since they determined the shape of the Taylor bubble by sketching the profile by hand, directly from the PIV image, they could not accurately define either the velocity field close to the interface or the bubble shape.

In the present study, a recent non-intrusive technique of Simultaneous Particle Image Velocimetry (PIV) and Pulsed Shadow Technique (PST) described in detail by Nogueira *et al.* [17] was applied to the hydrodynamic characterisation of the liquid film. Velocity profiles were obtained for the annular liquid film region around individual Taylor bubbles rising in a vertical tube of 32mm ID in stagnant and co-current flow conditions. Experiments were performed for a wide range of liquid viscosities ($2x10^{-3}$ Pa.s < μ < 0.2 Pa.s)

so that different flow regimes in the film can be quantitatively analysed.

EXPERIMENTAL SET-UP AND TECHNIQUE

Facility

The experimental study focused on the flow field characterisation in the annular film around a single Taylor bubble rising in a vertical column of stagnant and co-current liquid. The velocity fields were obtained applying simultaneously the Particle Image Velocimetry (PIV) and Pulsed Shadow Technique (PST). The experimental facility used is sketched in Fig.1 and is described in detail by Nogueira *et al.* [17].

The experiments were performed in a transparent acrylic column of 6-m height and 0.032-m internal diameter. The text section was located near the top of the tube to avoid entrance effects and to ensure a stabilized flow [11]. A box with plane faces surrounding the test section (0.5 m × 0.12 m × 0.11 m) was filled with the studied liquid in order to minimize the optical distortion.

The individual Taylor bubbles were generated and injected at the bottom of the column by manipulating valves 1 and 2. The volume of air used in these experiments varied between 40×10^{-6} m^3 and 265×10^{-6} m^3.

For the experiments in co-current conditions, the liquid flow rate was controlled by means of a peristaltic pump; in order to have a continuous flow rate in the test tube, a damping chamber was placed between the pump outlet and the column.

The system was thermally isolated and the difference of temperature, measured between thermocouples 1 and 2 (Fig. 1), was less than 0.3º C. The liquid viscosity at the temperature of each experiment was measured using a rotating Brookfield viscometer.

The test liquids were aqueous glycerol solutions covering the range of viscosities $2\times10^{-3}$to 0.22×10^{-3} Pa.s.

Measurement Techniques

To obtain the Taylor bubble velocity, two laser diodes separated by a distance of 0.25m were mounted perpendicularly to the tube pointing to two photocells placed in the opposite side of the column. The bubble velocity was obtained dividing the distance between the photocells by the time lag between the drop on their signals. The signal yielded by the photocell drops abruptly when the bubble passes between the laser diode and the photocell.

The PIV/PST technique consists of placing a board of light emitting diodes (LEDs) behind the test section pulsing simultaneously with the laser, so that a CCD camera (PCO camera with a resolution of 1280H x 1024V and 4096 grey levels) acquires an image containing both the PIV images and the bubble shadow. To obtain a close view of the liquid film, a lens of 50mm of focal length was used. Fluorescent particles (orange vinyl pigment, 10μm of mean size) were used as seeding. The particles remained dispersed in the test liquids after one day test. The same particles, emitting light at 590nm, were successfully used by Nogueira et al. [17] in their work. The particle size is of 0.6 pixels, while the particle image size is of around 4 pixels in the PIV images of the annular film.

A double-cavity pulsed Nd: Yag laser with a wavelength of 532 nm (pulse duration of 2.4 ns) and an adjustable pulse separation between each laser firing was used. The laser sheet had about 1-mm thickness in the test section. A red filter opaque below 550 nm, was used to block the intense green laser reflections and to allow the passage of the light emitted by the fluorescent particles and by the LEDs.

The synchronization between the laser, camera and LEDs was made using the same signal generator so that each frame of the camera recorded simultaneously a pulse of the LEDS and a pulse of the laser. The images obtained had three different grey levels corresponding to the seeding particles, background light and bubble shadow in descending order.

Data Processing

The images recorded with this technique contain both the PIV (flow field) and the PST (bubble shape) information. The processing is performed separately.

The flow field in the liquid was determined by processing the acquired images with the cross-correlation window-displacement - iterative - multigrid algorithm (WIDIM), developed by Scarano and Riethmuller [18]. In this process, the interrogation windows are displaced (according to the first vectors estimative) and their size is reduced iteratively. The use of a Gaussian interpolation function gives an estimate of the correlation peak location with sub-pixel accuracy. In this work the initial window size is of 64 × 32 pixels, according to the privileged flow direction. Two refinements are performed to reach final interrogation windows of 16 × 8 pixels. An overlap of 50% refines the grid spacing to 8 × 4 pixels and allows a resolution of 0.138 mm × 0.069 mm ($0.04d \times 0.02d$) in the measurements performed in the annular liquid film. The time between the pulsing of the two laser cavities (pulse separation) was adjusted according to the measured velocities for the entire range of studied conditions and varied from 120 μs to 2000 μs. The spurious vectors identification was made, eliminating vectors with a signal to noise ratio (SN) less than 1.5. Interpolated vectors from the neighbours substituted these vectors. The average SN in a processed image was around 10. As a result of the PIV processing some wrong vectors appear inside the bubble resulting from erroneous particle images corresponding to refraction and reflection of the light emitted by the particles, as explained by Nogueira *et al*. [17] The elimination of these optical effects by using simultaneous PIV and PST, allows the determination of the exact position of the interface, i.e. the bubble shape. The determination of the shadow of the bubble is obtained according to a procedure described in detail by Nogueira *et al*. [17].

It is largely accepted that the main uncertainty associated with PIV measurements is less than a tenth of a pixel. The high resolution allowed by the PCO camera used leads to an estimated overall uncertainty of 1.5%.

RESULTS

In the present work the flow field in the annular film of individual Taylor bubbles rising through stagnant and co-current liquids in vertical tubes was studied. Experiments were performed with aqueous glycerol solutions with viscosities in the range $2\text{x}10^{-3}$ Pa.s < μ <0.22 Pa.s. The presented data were processed as explained in detail

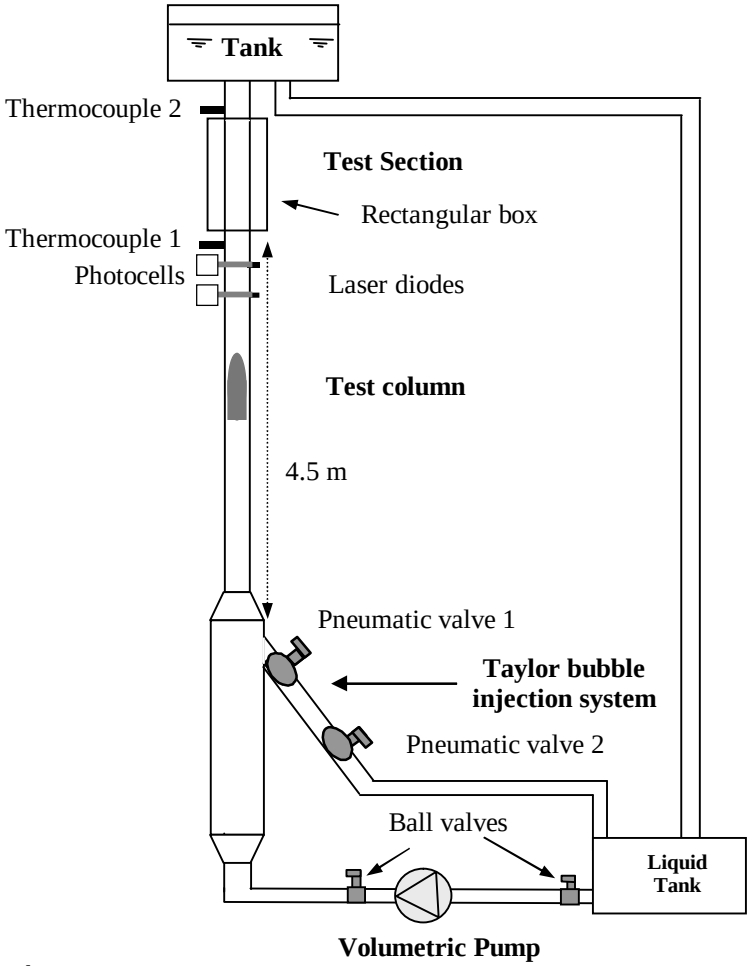

Figure 1 – Experimental Facility

by Nogueira *et al.*[17]. The experimental conditions studied are summarised in Table 1.

Table 1 – Experimental Conditions

μ (Pa.s)	ρ (kg/m^3)	T (°C)	U_B (m/s)	$\delta_{exp}\times10^3$ (m)	$Re_{u\delta}$	S/C
0.205	1232.4	19.7	0.303	3.87	40	C
0.190	1232.8	20.8	0.189	3.78	42	S
0.111	1222.2	20.2	0.197	3.29	94	S
0.459	1201.9	19.8	0.226	2.48	366	C
0.433	1200.4	21.0	0.197	2.36	395	S
0.448	1201.3	20.9	0.390	2.71	415	C
0.144	1170.0	21.8	0.380	2.58	1213	C
0.139	1169.7	22.7	0.360	2.40	1475	C
0.144	1169.9	21.8	0.197	1.84	1630	S
0.024	1071.4	18.4	0.197	1.62	10706	S

The liquid flowing around the Taylor bubble accelerates downwards in the nose region and creates a thin liquid film. The maximum liquid velocity in the axial direction in a given cross section approaches the bubble interface until the point where the forces acting on a liquid element are in balance. The velocity profile becomes fully developed and consequently the film thickness, *d*, reaches a constant minimum value. This is well brought out in Figure 2 representing the flow in the developing film region around a Taylor bubble rising in a stagnant glycerol solution (μ = 0.19 Pa.s), in a fixed frame of reference.

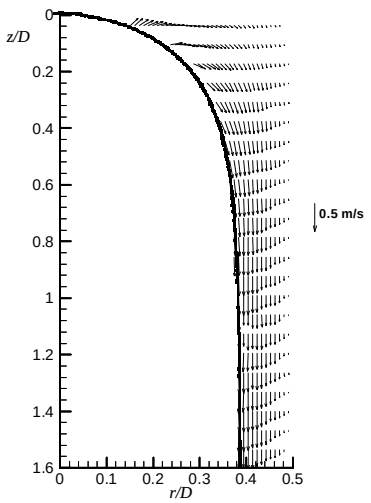

Figure 2 – Velocity profile in the developing film region around a Taylor bubble rising in a stagnant liquid (μ =0.19 Pa.s) in a fixed frame of reference

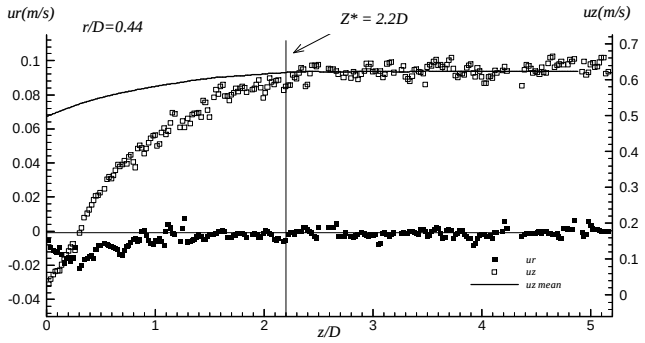

(a) stagnant conditions

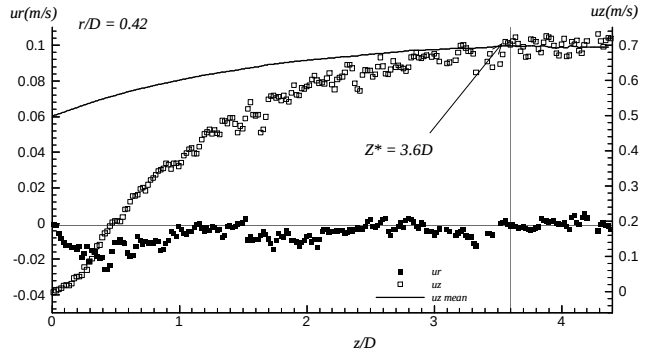

(b) co-current conditions

Figure 3 – Axial, radial and mean axial components of the velocity in the liquid film

In Figures 3a and 3b the axial, (u_z) and radial, (u_r), components of the liquid velocity along the annular film are represented for a radial position of r/D = 0.44 in (a) stagnant conditions and of r/D = 0.42 for co-current (b) conditions. The origin of the axial coordinate z is taken at the bubble nose. In the Figures are also plotted, for each axial position along the film, the mean value of u_z, $u_{z_{mean}}$, over the entire film below that axial position until around 6D. The represented data were obtained from several consecutive PIV images 'stiched' together in order to study the entire film.

The axial velocity component increases along the film until it gets fully developed, i.e. when the film reaches a constant thickness. For the represented experimental conditions, values for the length of developing film, Z*, were estimated: about 2.2 D for stagnant liquid and about 3.6 D for co-current flowing liquid. The radial component of the film velocity reaches a value around zero (fully developed film) for the same values of Z*. The same developing lengths were found analysing the values of $u_{z_{mean}}$ since they reach a constant value for the same values of Z*.

A theoretical estimate of the length Z* for which the boundary layer from the wall reaches the free streamline along the bubble interface can, as reported by Campos and Guedes de Carvalho [8], be given by

$$Z^* \approx \frac{\left[\left(gd^2/2n\right)+U_B\right]}{2g} \qquad (1)$$

where U_B is the Taylor bubble velocity, g the acceleration due to gravity and ν the kinematic viscosity. This equation was deduced applying Bernoulli's equation along the free streamline and supposing unidirectional flow in a liquid layer with a free surface in a vertical plate. Equation (1) can be rewritten in a dimensionless form giving

$$\frac{Z^*}{D} \approx \left[3\frac{\mathrm{Re}_{vd}}{x} - 0.5\frac{\mathrm{Re}_F}{(1-x)^2}\right]^2 \frac{1}{2N_f{}^2} \qquad (2)$$

where $x = 2d/D$ is the dimensionless film thickness, $\mathrm{Re}_F = \frac{U_B(D-2d)^2}{nD}$ is the film Reynolds number based on the bubble velocity, $\mathrm{Re}_{vd} = \frac{v_d d}{n}$ is the film Reynolds number based on the average liquid film velocity relative to the bubble, v_d, and $N_f = \frac{\left(gD^3\right)^{1/2}}{n}$ the inverse viscosity number. In Figure 4 the ratio between experimental values of Z^*/D and the predictions of Eq. (2), is represented against the Reynolds number based on the absolute average velocity in the liquid film, Re_{u_d}, for the studied conditions. As depicted in the Figure, Eq. (2) under predicts the film developing length for low values of Re_{u_d}. This is probably due to the consideration of inviscid flow when deducing Eq. (1). For intermediate values of Re_{u_d} the theory seems to predict well the developing length. Above values of Re_{u_d} around 400, the experimental values are lower than predictions, which seems to indicate the occurrence of transition from laminar to turbulent regime in the film flow.

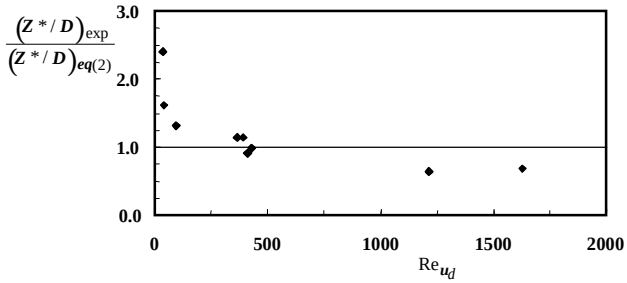

Figure 4 – Comparison between the predicted and experimental values of Z^*/D

Brown [5] theoretically deduced an expression for the velocity profile in a stabilized free laminar falling film around a Taylor bubble rising trough a co-current flowing liquid (mean superficial velocity U_L):

$$u = \frac{g}{n}\left[\frac{R^2 - r^2}{4} - \frac{(R-d)^2}{2}\ln\frac{R}{r}\right] \qquad (3)$$

where the film thickness, d, is given by

$$d = \left[\frac{3n}{2g(R-d)} \left((R-d)^2 U_B - R^2 U_L \right) \right]^{1/3} \quad (4)$$

Figures 5a) and 5b) show the average developed velocity profiles in the annular film for the stagnant conditions, ($U_L = 0$), and for the co-current conditions studied, respectively. The experimental profiles represent the average of 60 instantaneous profiles along the stabilised film. The lines represent for each experiment the theoretical laminar profile given by Eq. (3) using the film thickness predicted by Eq. (4).

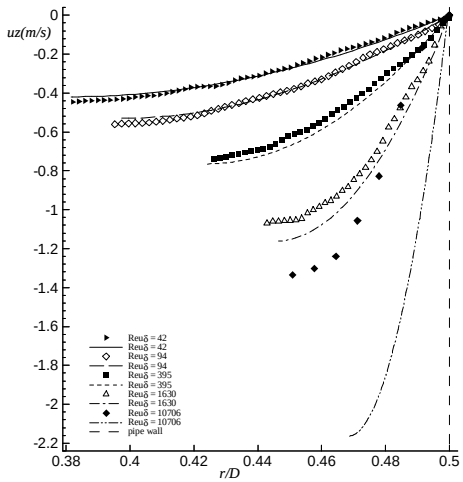

(a) stagnant conditions

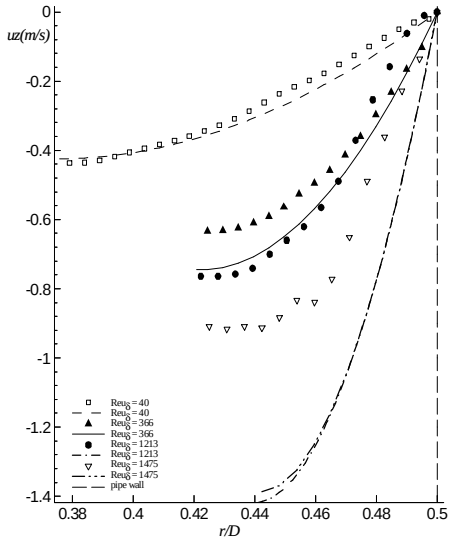

(b) co-current conditions

Figure 5 – Average of the axial component of the velocity in the liquid falling film for the studied conditions. The lines represent the theoretical profiles for laminar regime (Brown [5])

For each condition, the average experimental profile is plotted within the film thickness determined by the bubble shadow. As depicted in the figures the experimental film thickness decreases as the Reynolds number based on the absolute average velocity in the liquid film, Re_{u_d}, increases, as expected. For low values of Re_{u_d}, corresponding to laminar regime, Eq. (4) predicts very well the film thickness (deviations below 3%). For values of Re_{u_d} greater than around 400, the deviations between the theoretical and experimental thicknesses become reasonable (greater than 20%), suggesting the transition of the flow regime in the film. A similar conclusion arises from the comparison between the experimental velocity profiles and predictions from Brown's equation. Finally, the plot of Figure 6 reinforces this feature. It is possible to confirm the occurrence of transition from laminar to turbulent regime in the annular film at values of Re_{u_d} around 400. From there on the ratio between the experimental values of d and the predictions from Eq. (4) becomes significantly different from one.

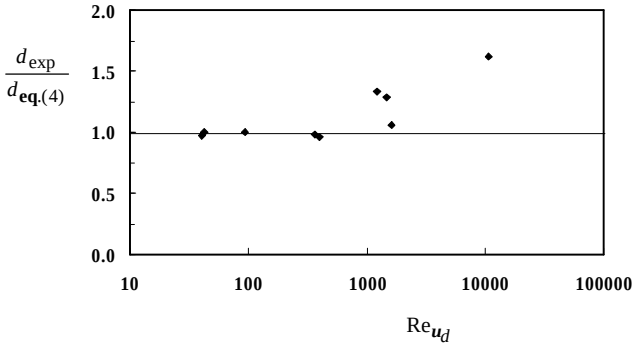

Figure 6 – Comparison between experimental values of the film thickness and the predictions from eq.(4).

More data are presently being determined for accurately define the transition region.

CONCLUSIONS

The flow in the annular film around individual Taylor bubbles rising in vertical columns of stagant and co-current liquids was quantitatively studied by means of a non-intrusive technique using particle image velocimetry and shadowgraphy.

The velocity profiles near the nose region indicate free falling film in the initial stages of film formation. Further down, the velocity profiles are characteristic of a falling film flow. Accordingly, the film thickness, d, is constant in the fully developed region.

Values for the dimensionless developing film length are reported and compared with theoretical predictions supposing inviscid flow in the nose region. For values of the Reynolds number based on the mean absolute velocity in the liquid film, Re_{u_d}, greater than around 400, the experimental values for the developing length become lower than the predictions, suggesting the occurence of transition from laminar to turbulent regime. Accordingly, the experimental velocity profiles are characteristic of developed laminar falling film until values of Re_{u_d} around 400. Also the determined experimental values of the film thickness are well predicted by laminar falling film theory in the same range of Re_{u_d}. Although further data are needed to accurately define the critical Reynolds number, the value of 400 is suggested in this study. The data

reported are relevant for the validation of numerical simulations in slug flow.

ACKNOWLEDGMENT

The partial support given by FCT through project POCTI/EQU/33761/1999 and scholarship BD/20301/99 is gratefully acknowledged. POCTI (FEDER) also supported this work via CEFT.

NOMENCLATURE

C	co-current conditions (Table 1)
D	internal column diameter, m
g	acceleration due to gravity, $m.s^{-2}$
r	radial position, m
R	internal column radius, m
S	stagnant conditions (Table 1)
U_B	Taylor bubble velocity, $m.s^{-1}$
U_L	mean superficial liquid velocity, $m.s^{-1}$
u_r	radial component of the velocity, $m.s^{-1}$
u_z	axial component of the velocity, $m.s^{-1}$
$u_{z_{mean}}$	mean values of u_z below an axial position, $m.s^{-1}$
u_d	liquid average velocity in the film relative to the tube wall, $m.s^{-1}$
v_d	liquid average velocity in the film relative to the bubble, $m.s^{-1}$
z	distance from the Taylor bubble nose, m
Z^*	distance from the Taylor bubble nose for which the annular liquid film stabilizes or film developing length, m

Dimensionless groups

N_f	Inverse viscosity number $\left(=\frac{g^{1/2}D^{3/2}}{n}\right)$
Re_f	Reynolds number based on the bubble velocity, $\left(=\frac{U_B(D-2d)^2}{nD}\right)$
Re_{u_d}	Reynolds number based on the mean absolute velocity in the liquid film $\left(=\frac{u_d D}{n}\right)$
Re_{v_d}	Reynolds number based on the mean velocity in the liquid film relative to the bubble $\left(=\frac{v_d D}{n}\right)$
x	dimensionless film thickness
$\frac{Z^*}{D}$	dimensionless film developing thickness
$\left(\frac{Z^*}{D}\right)_{\exp}$	experimental values of the dimensionless film developing thickness
$\left(\frac{Z^*}{D}\right)_{eq.2}$	theoretical predictions of the dimensionless film developing thickness

Greek letters

d	liquid film thickness, m
$d_{\exp}$	experimental values of the liquid film thickness, m
$d_{eq.4}$	theoretical predictions of the liquid film thickness, m
n	liquid kinematic viscosity, $m^2.s^{-1}$
m	liquid dynamic viscosity, Pa.s
r	liquid density, $kg.m^{-3}$

REFERENCES

1. D. T. Dumitrescu. Stromung an Einer Luftblase im Senkrechten Rohr, *Z. Angeus. Math. Mec.*, **23**, 139-149, 1943.
2. E. T. White and R. H. Beardmore. The Velocity of Single Cylindrical Air Bubbles Through Liquids Contained in Vertical Tubes, *Chem. Engng Sci.*, **17**, 351-361, 1962.
3. D. J. Nicklin, J. O. Wilkes and J. F. Davidson. Two-Phase Flow in Vertical Tubes, *Trans. Inst. Chem. Engrs.*, **40**, 61-68, 1962.
4. R. Moissis and P. Griffith. Entrance effects in a two-phase slug flow, *J. Heat Transfer*, **84**, 29-39, 1962.
5. R. A. S. Brown, The Mechanism of Large Bubbles in tubes. I. Bubble velocities in stagnant liquids. *Can. J. Chem. Engng*, **43**, 217-223, 1965.
6. R. Collins, F. F. De Moraes, J. F. Davidson and D. Harrison. The Motion of Large Gas Bubble Rising Through Liquid Flowing in a Tube, *J. Fluid Mech.*, **28**, 97-112, 1978.
7. R. C. Fernandes, R. Semiat and A. E. Dukler. A Hydrodynamic Model for Gas-Liquid Slug Flow in Vertical Tubes, *AIChE J.*, **29**, 981, 1983.
8. J. B. L. M. Campos and J. R. F. Guedes de Carvalho. An Experimental Study of the Wake of Gas Slugs Rising in Viscous Liquids, *J. Fluid Mech.*, **196**, 27-37, 1988.
9. Z. S. Mao and A. E. Duckler. The motion of Taylor Bubbles in Vertical Tubes: II. Experimental Data and Simulations for Laminar and Turbulent Flow, *Chem. Eng. Sci,*, **46**, 2055-2064, 1991.
10. A. M. F. R. Pinto and J. B. L. M. Campos. Coalescence of Two Gas Slugs Rising in a Vertical Column of Liquid, *Chem. Engng Sci.*, **51**, 45-54, 1996.
11. A. M. F. R. Pinto, M. N. Coelho Pinheiro and J. B. L. M. Campos. Coalescence of Two Gas Slugs Rising in a Co-Current Flowing Liquid in Vertical Tubes, *Chem. Engng Sci.*, **53**, 2973-2983, 1998.
12. A. M. F. R. Pinto, M. N. Coelho Pinheiro and J. B. L. M. Campos. On the Interaction of Taylor Bubbles Rising in Two-phase Co-current Slug Flow in Vertical Columns, *Exp. in Fluids*, **31**, 643-652, 2001.
13. J. Fabre and A. Liné. Modeling of Two-Phase Slug Flow, *Annu. Rev. Fluid Mech*, **24**, 21-46, 1992.
14. S., Polonsky, L. Shemer, and D. Barnea, The relation between the Taylor bubble motion and the velocity

field ahead of it. *Int. J. Multiphase Flow*, **25**, 957-975, 1999

15. R. van Hout, A. Gulitsky, D. Barnea and L. Shemer. Experimental investigation of the velocity field induced by a Taylor bubble rising in stagnant water. *Int. J. Multiphase Flow*, **29**, 579-596, 2002
16. W. Bugg, J. D. and Saad, G. A. The velocity field around a Taylor bubble rising in a stagnant viscous fluid: numerical and experimental results. *Int. J. Multiphase Flow*, **28**, 791-803, 2002.
17. S. Nogueira, R. G. Sousa, A, M. F. R. Pinto, M. L. Riethmuller and J. B. L. M. Campos, Simultaneous PIV and Pulsed Shadow Technique in Slug Flow: a Solution for Optical Problems. *Exp. in Fluids*, **35**, 598-609, 2003
18. F. Scarano and M. L. Riethmuller. Iterative multigrid approach in PIV image processing with discrete window offset. *Exp. Fluids.* **26**, 513-523, 1999